Supplemental Figures

Figure Legends

Figure S1

(A-B) EHBP-1 interacts with RAB-10. RAB-10(Q68L) and RAB-10(T23N) were expressed in a yeast reporter strain as a fusion with the DNA-binding domain of LexA (bait). EHBP-1 (aa 443-901) was expressed in the same yeast cells as a fusion with the B42 transcriptional activation domain (prey). Interaction between bait and prey was assayed by β-Galactosidase color assay without galactose–induction (A) and with galactose-induction (B). Two independent colonies were assayed. The asterisk "*" indicates a positive interaction.

(C-D) Full length EHBP-1 does not interact with full length RME-1 or the isolated RME-1 EH-domain. (C) Interaction between bait and prey was assayed by β-Galactosidase color assay without galactose–induction and with galactose-induction. (D) Interaction between bait and prey was assayed by complementation of leucine auxotrophy (LEU2 growth assay). Two independent colonies were assayed for each condition.

Figure S2 RAB-8(Q67L) interacts with the EHBP-1 C-terminal predicted coiled-coil region (aa 712-851). RAB-8(Q67L) was expressed in a yeast reporter strain as a fusion with the DNA-binding domain of LexA (bait). EHBP-1 (aa 712-851) was expressed in the same yeast cells as a fusion with the B42 transcriptional activation domain (prey). Interaction between bait and prey was assayed by complementation of leucine

auxotrophy (LEU2 growth assay). Colonies were diluted in liquid and spotted on solid growth medium directly or after further 0.1X dilution.

Figure S3 (A) Amino acid sequence alignment of Ehbp1 orthologs: *H. sapiens* (ENSEMBL:ENSP00000346482), *M. musculus* (SW:Q69ZW3), *D. melanogaster* (FLYBASE:CG15609), *C. briggsae* (FLYBASE:CG15609) and *C. elegans* (WP:CE05711). The sequence alignment was created and refined using Clustal W 1.83 (EMBL-EBI, UK) followed by Boxshade3.21 (Swiss Node, EMBnet). Identical amino acids are shaded in blue; NPF motifs are shaded in pink. (B-C) Schematic representations of protein domains in (B) EHBP-1 and (C) MICAL-L1. Protein domains are displayed as dark boxes above protein sequence (shown as dark lines). Amino acid numbers are indicated.

Figure S4 (A-B") RAB-10 colocalizes with RAB-8 on endosomes. All images are from deconvolved 3-D image stacks acquired in intact living animals expressing GFP and RFP- tagged proteins in the intestinal epithelial cells. (A-A") GFP-RAB-10 colocalizes extensively with RFP-RAB-8 on endosomes near the intestine basolateral membrane. Arrowheads indicate endosomes labeled by both GFP-RAB-10 and RFP-RAB-8. (B-B") GFP-RAB-10 partially colocalizes with RFP-RAB-8 on endosomal structures deep in intestinal cytosol. Arrowheads indicate endosomes labeled by both GFP-RAB-10 and RFP-RAB-8. In each image autofluorescent lysosome-like organelles can be seen in all three channels with the strongest signal in blue, whereas GFP appears only in the green channel and RFP only in the red channel. Signals observed in the green or red channels

that do not overlap with signals in the blue channel are considered bone fide GFP or RFP signals, respectively. Scale bar represents 10 μm.

(C-D) Nomarski images of the intestines in *ehbp-1(tm2523)* mutants and *ehbp-1(tm2523)* animals with intestine specific transgenic expression of EHBP-1-GFP. Large transparent vacuoles were found in the intestines of *ehbp-1(tm2523)* animals (C). The vacuolation phenotype could be rescued by intestine specific expression of EHBP-1-GFP (D-D'). Scale bar represents 10 μm.

Figure S5 Over-expression of mutant form of EHBP-1(aa1-711) lacking RAB-10 interacting coiled-coil region induced dominant negative phenotypes. In wild-type animals, hTAC-GFP colocalized with full-length EHBP-1-mCherry on tubules and small puncta (A-A"). Over-expression of EHBP-1(aa1-711) induced intracellular accumulation of hTAC-GFP that colocalized with EHBP-1(aa1-711)-mCherry (B-B"). In each image autofluorescent lysosome-like organelles can be seen in all three channels with the strongest signal in blue, whereas GFP appears only in the green channel and mCherry only in the red channel. Signals observed in the green or red channels that do not overlap with signals in the blue channel are considered bone fide GFP or mCherry signals, respectively.

(C-F) Dominant negative phenotypes induced by expression of EHBP-1(aa1-711). Over-accumulation of intracellular hTAC-GFP in animals with transgenic over-expression of EHBP-1(aa1-711)-mCherry (C-E). (F) Nomarski image of the intestine in animal with transgenic over-expression of EHBP-1(aa1-711)-mCherry. Arrow indicates the grossly

enlarged endosomal structure. Error bars are SEM (n=18 each, 6 animals of each genotype sampled in three different regions of each intestine). Asterisks indicate a significant difference in the one-tailed Student's t-test ($p<0.001$). Scale bar represents 10 μm.

Figure S6 *ehbp-1* RNAi knockdown does not affect GFP-RAB-11 subcellular distribution. Confocal images in a wild-type and *ehbp-1(RNAi)* animals are shown for GFP-RAB-11 expressed in the intestine. Scale bar represents 10 μm.

Figure S7 EHBP-1-labeled endosomal morphology is perturbed in *rab-10(q373)* mutants (C), but not after *rab-8* RNAi (B). Depletion of RAB-8 in rab-10(q373) mutants did not enhance the EHBP-1-labeled endosome morphology defect (D). Arrowheads indicate enlarged endosomes labeled by EHBP-1-GFP (C-D). Scale bar represents 10 μm.

Figure S8 RAB-8-labeled endosomes over-accumulate in *ehbp-1(RNAi)*, *rab-10(q373),* and *rme-1(b1045)* animals (A-D, E). Representative confocal images of animals are shown for GFP-RAB-8 (A-D) and average total intensity of GFP-RAB-8 per unit area was quantified in (E). Error bars are SEM (n=18 each, 6 animals of each genotype sampled in three different regions of each intestine). Asterisks indicate a significant difference in the one-tailed Student's t-test ($p<0.001$). Scale bar represents 10 μm.

Figure S9 Analysis of RAB-8 function in GLR-1 glutamate receptor trafficking. GLR-1-GFP fluorescence was observed along ventral cord neurites of (A) wild-type animals and (B) *rab-8(tm2526)* mutants. In both wild-type animals and *rab-8* mutants, GLR-1-GFP is localized to small (~0.5 μm) synaptic puncta. Occasionally, *rab-8* mutants accumulate GLR-1-GFP in elongated (~2-3 μm) accretions (arrows) similar to those observed in *rab-10* and *ehbp-1* mutants, but smaller and less numerous. The (C) mean number (per 100 μm of ventral cord) and (D) size (length in μm) of GLR-1GFP accretions is plotted. The (E) mean number of GLR-1-GFP puncta (per 100 μm of ventral cord) and (F) size (in μm) is also plotted. (G) The mean spontaneous reversal frequency (number of reversals per minute over a 5-min period) is plotted for the given genotype. Unlike *rab-10* and *ehbp-1* mutants, *rab-8* mutants reverse with a frequency similar to that of wild type. (H) GLR-1-GFP (green) and mRFP-RAB-8 (red) are shown co-expressed in the same interneurons via the *glr-1* promoter. Puncta of mRFP-RAB-8 accumulate both within and proximal to the neuron cell bodies (arrows); however, unlike EHBP-1 and RAB-10, mRFP-RAB-8 is found diffusely distributed throughout the rest of the ventral cord neurites. Scale bar represents 5 μm. Error bars are SEM (N= 21–40 animals for each genotype). $*p < 0.05$, $***p < 0.01$ by analysis of variance (ANOVA) followed by Dunnett's multiple comparison to wild type.

Figure S10 (A-E) Nomarski images of the gonads in wild type, *rab-10(q373)*, *rab-8(RNAi)*, *rab-10(q373)*;*rab-8(RNAi)*, and *ehbp-1(tm2523)* animals. Developmental defects of gonads were found in *rab-10(q373)*;*rab-8(RNAi)* animals and *ehbp-1(tm2523)* mutants (D-E). Arrows indicate the normal large squared-off oocyte cells in the proximal

gonad region (A-C) and the lack of the characteristic row of oocyte cells in the proximal gonad regions (D-E). Scale bar represents 10 μm.

Figure S11 Diagram of *C. elegans* germline organization.

Functional analysis of GFP-SNB-1 localization was assayed in the boxed region.

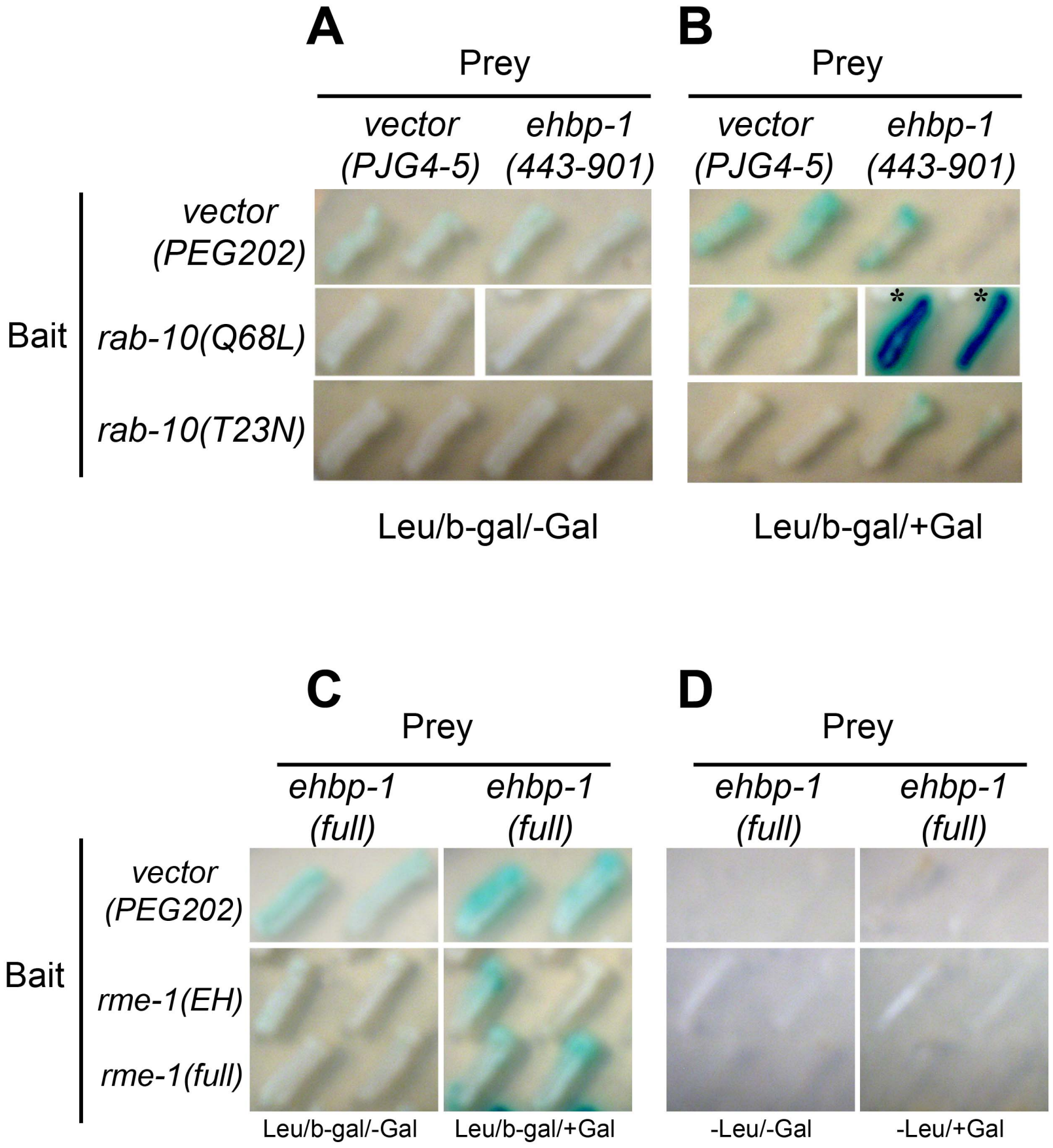
A
Prey
vector (PJG4-5)
ehbp-1 (443-901)
Bait
vector (PEG202)
rab-10(Q68L)
rab-10(T23N)
Leu/b-gal/-Gal
B
Prey
vector (PJG4-5)
ehbp-1 (443-901)
*
*
Leu/b-gal/+Gal
C
Prey
ehbp-1 (full)
ehbp-1 (full)
Bait
vector (PEG202)
rme-1(EH)
rme-1(full)
Leu/b-gal/-Gal
Leu/b-gal/+Gal
D
Prey
ehbp-1 (full)
ehbp-1 (full)
-Leu/-Gal
-Leu/+Gal

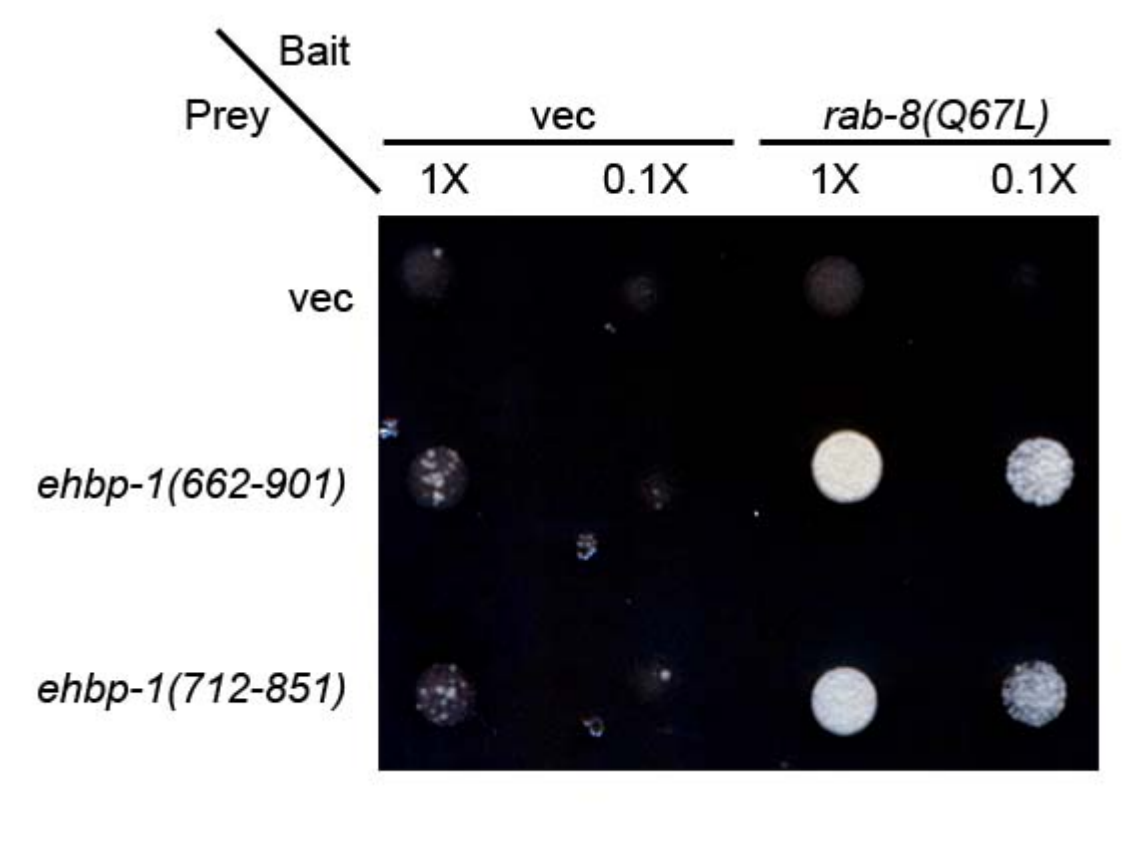
Bait
Prey
vec
rab-8(Q67L)
1X
0.1X
1X
0.1X
vec
ehbp-1(662-901)
ehbp-1(712-851)

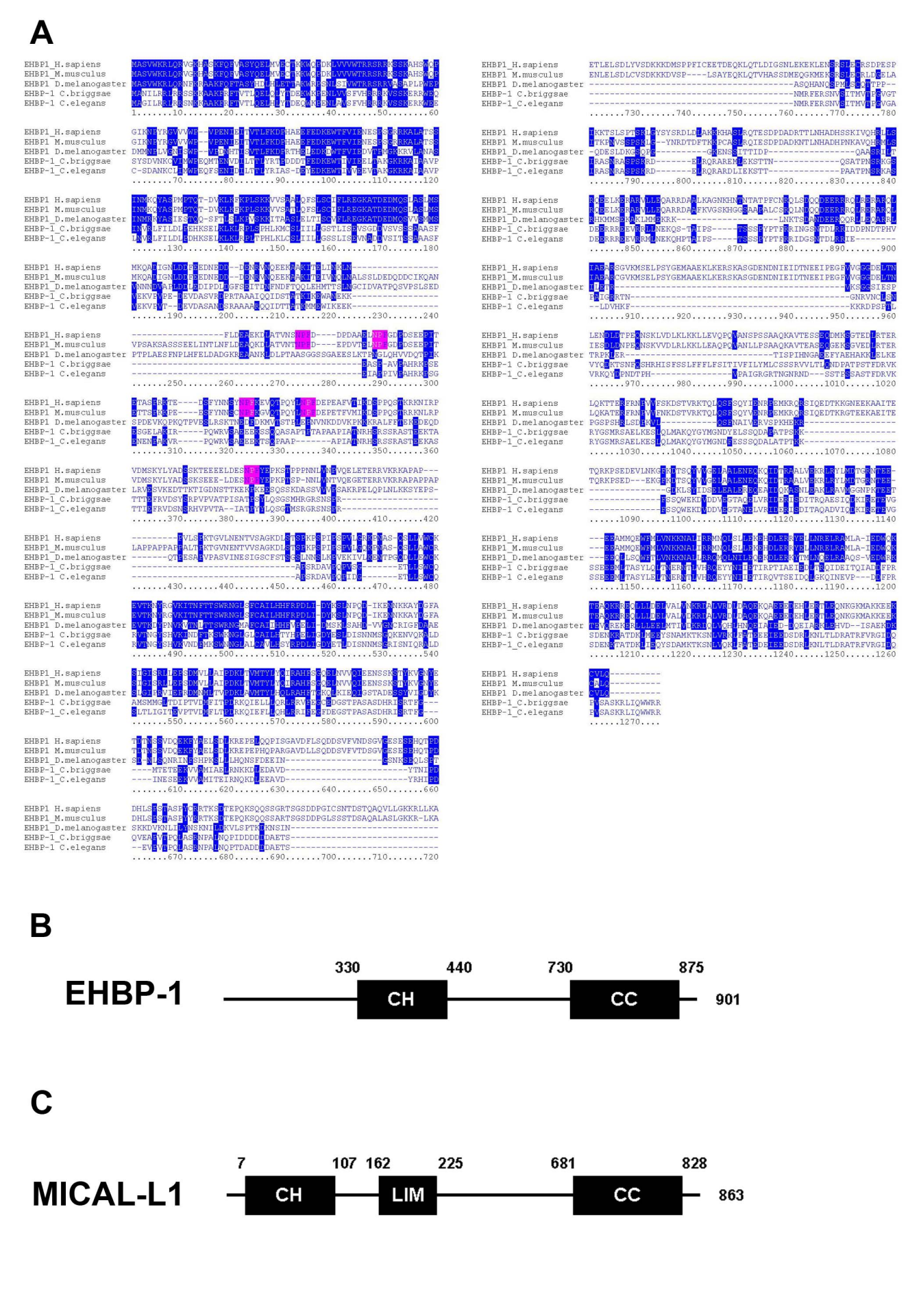
A
EHBP1_H.sapiens
EHBP1_M.musculus
EHBP1_D.melanogaster
EHBP-1 C.briggsae
EHBP-1 C.elegans
B
EHBP-1
330
440
730
875
901
CH
CC
C
MICAL-L1
7
107
162
225
681
828
863
CH
LIM
CC

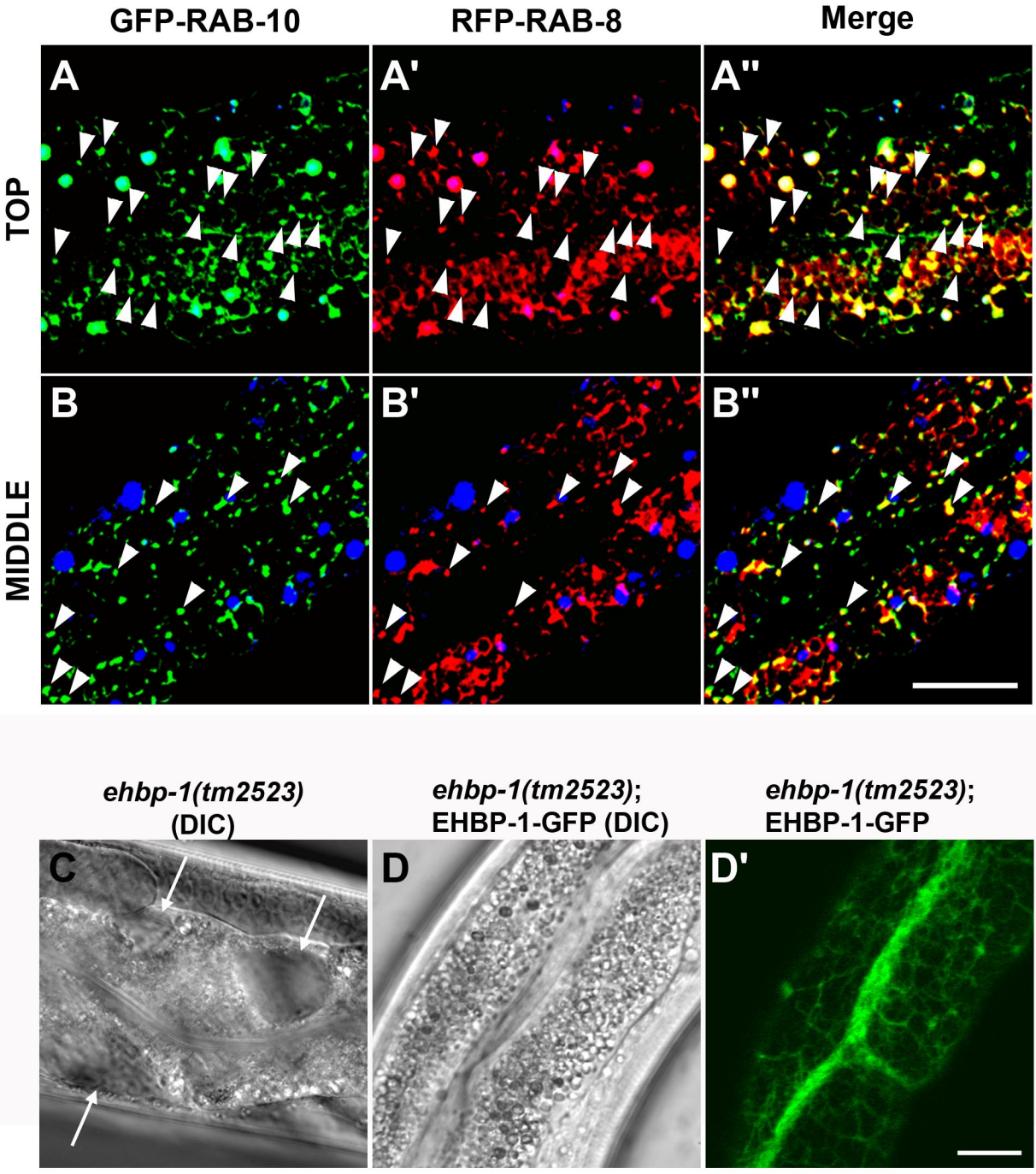
GFP-RAB-10
RFP-RAB-8
Merge
TOP
MIDDLE
A
A'
A''
B
B'
B''
ehbp-1(tm2523)
(DIC)
ehbp-1(tm2523);
EHBP-1-GFP (DIC)
ehbp-1(tm2523);
EHBP-1-GFP
C
D
D'

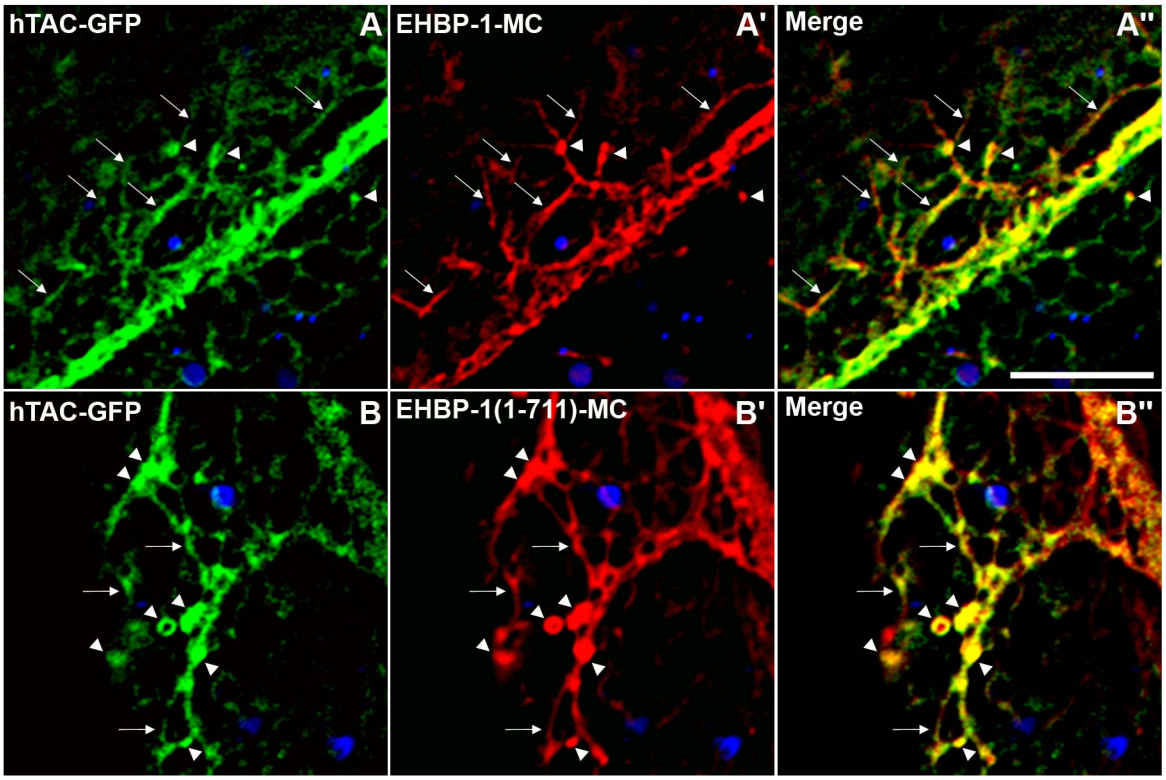
hTAC-GFP
A
EHBP-1-MC
A'
Merge
A''
hTAC-GFP
B
EHBP-1(1-711)-MC
B'
Merge
B''

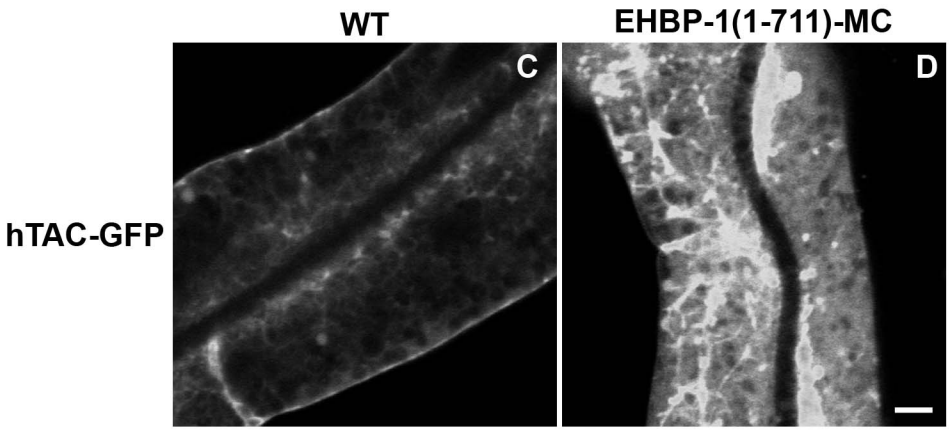
WT
EHBP-1(1-711)-MC
hTAC-GFP
C
D

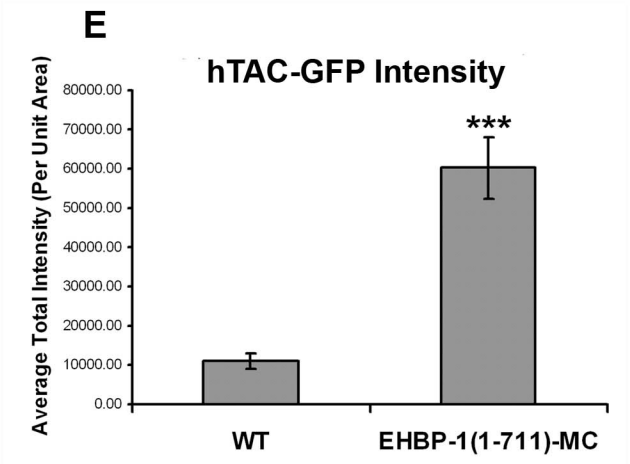
E
hTAC-GFP Intensity
Average Total Intensity (Per Unit Area)
80000.00
70000.00
60000.00
50000.00
40000.00
30000.00
20000.00
10000.00
0.00
***
WT
EHBP-1(1-711)-MC

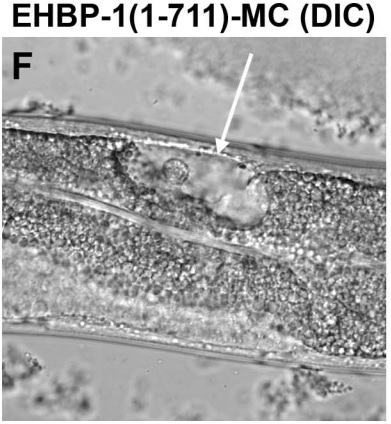
EHBP-1(1-711)-MC (DIC)
F

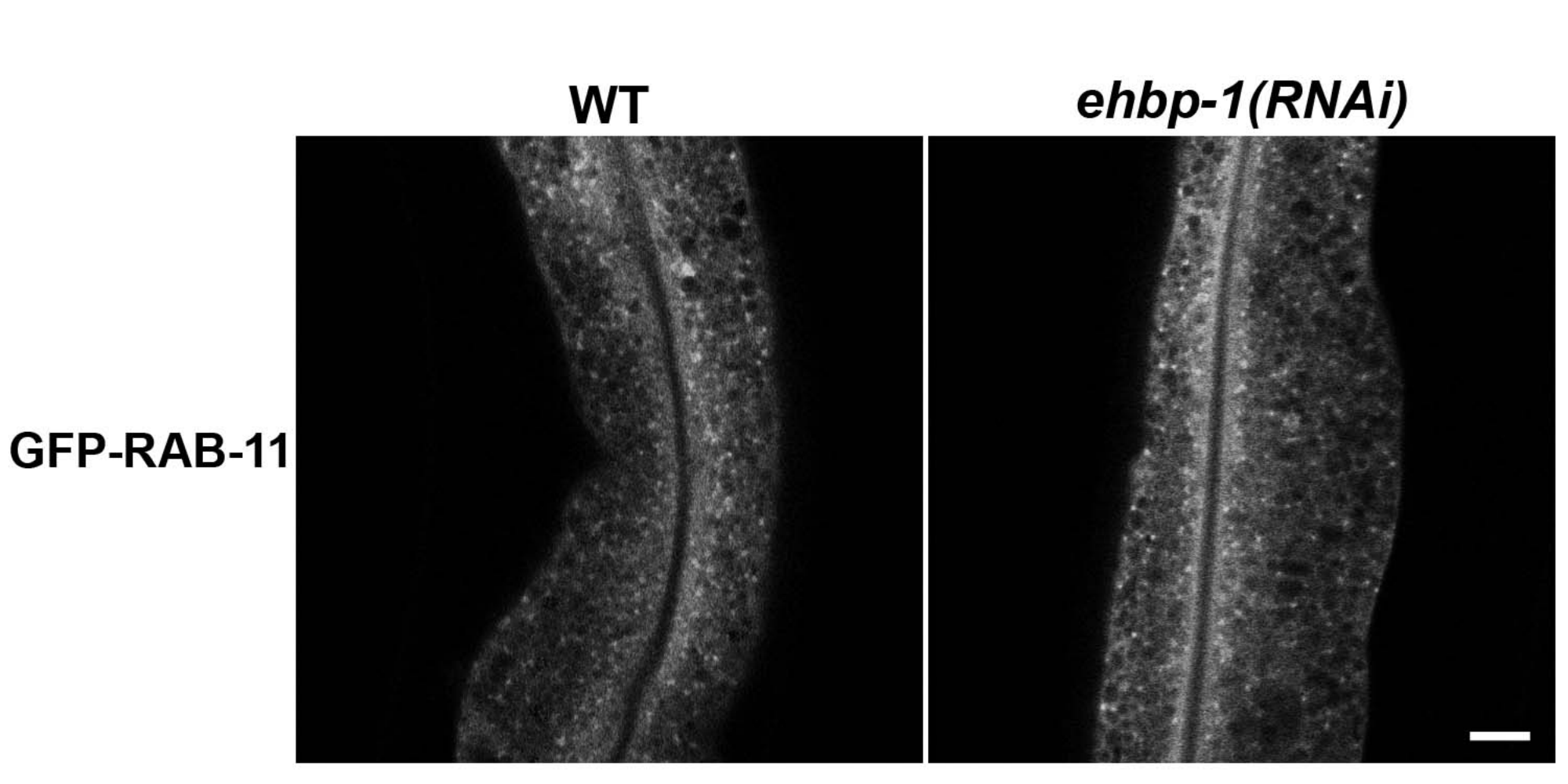
WT
ehbp-1(RNAi)
GFP-RAB-11

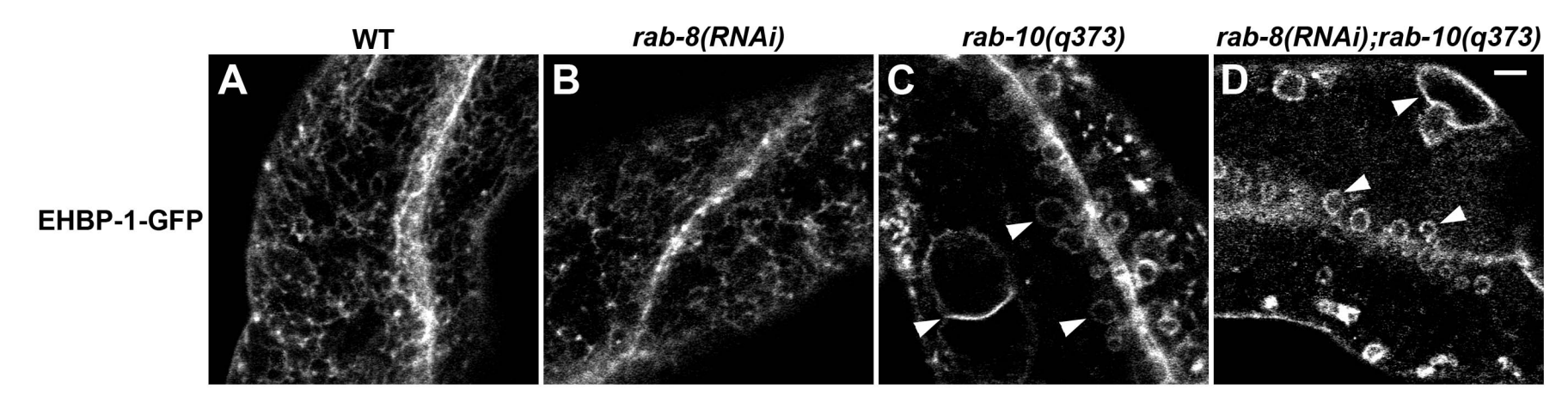
WT
rab-8(RNAi)
rab-10(q373)
rab-8(RNAi);rab-10(q373)
EHBP-1-GFP
A
B
C
D

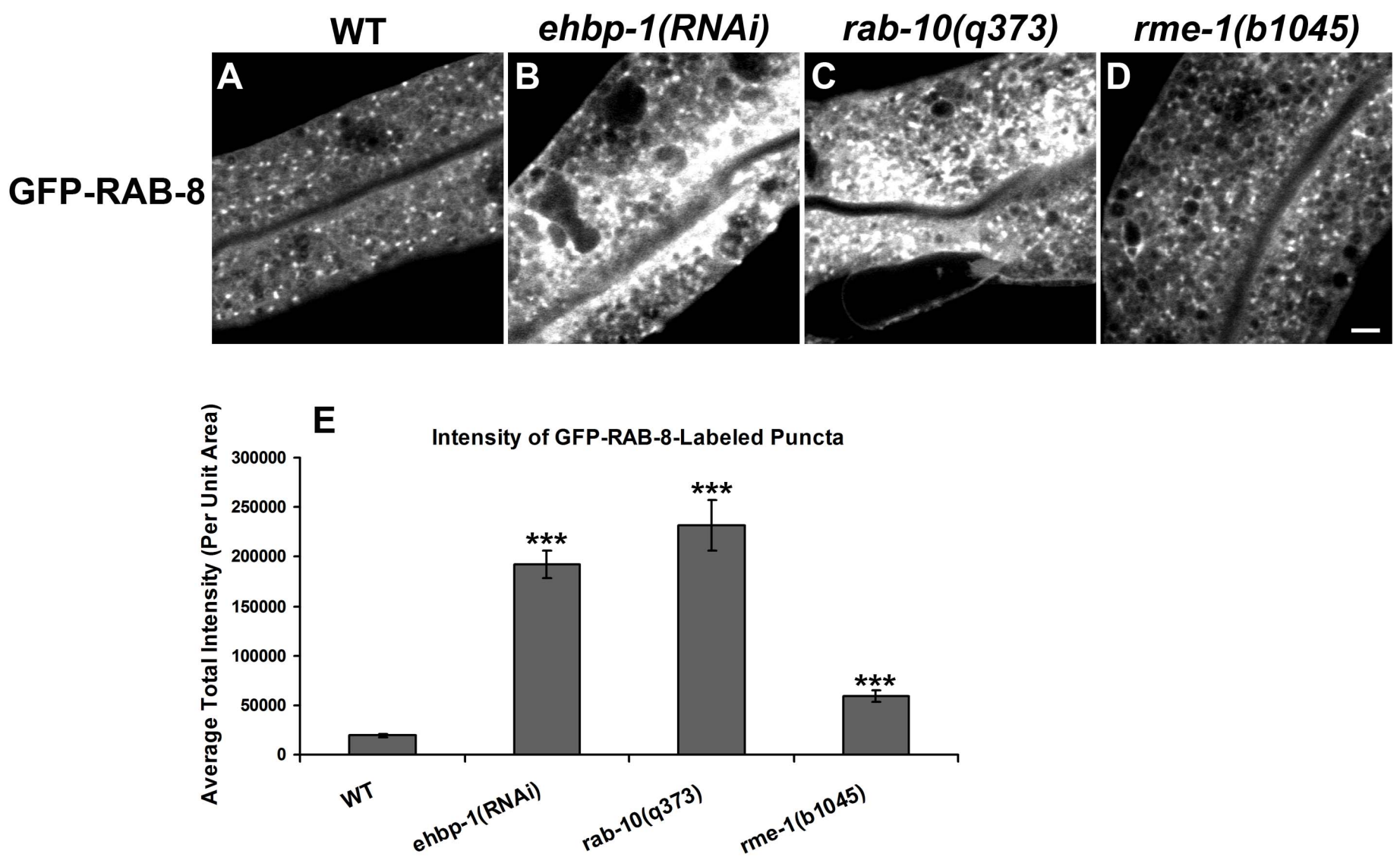
WT
ehbp-1(RNAi)
rab-10(q373)
rme-1(b1045)
GFP-RAB-8
A
B
C
D
E
Intensity of GFP-RAB-8-Labeled Puncta
Average Total Intensity (Per Unit Area)
300000
250000
200000
150000
100000
50000
0
***
***
***
WT
ehbp-1(RNAi)
rab-10(q373)
rme-1(b1045)

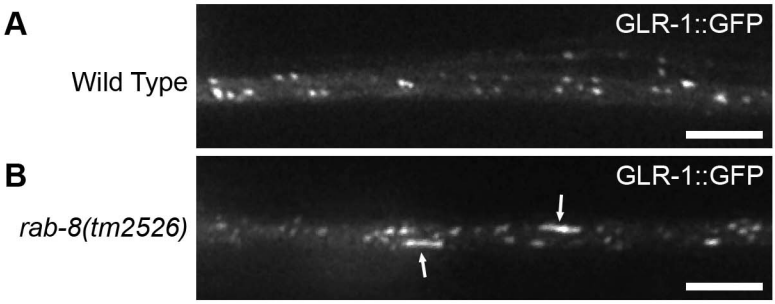
A
Wild Type
GLR-1::GFP
B
rab-8(tm2526)
GLR-1::GFP

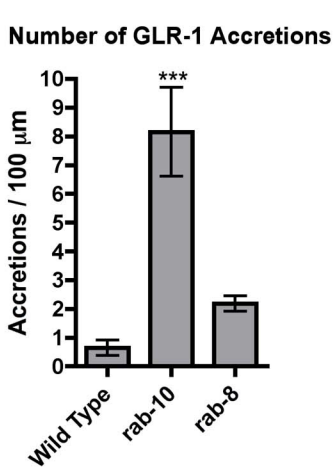
C
Number of GLR-1 Accretions
Accretions / 100 µm
***
Wild Type
rab-10
rab-8

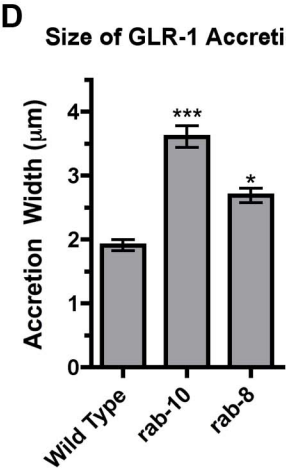
D
Size of GLR-1 Accretions
Accretion Width (µm)
***
*
Wild Type
rab-10
rab-8

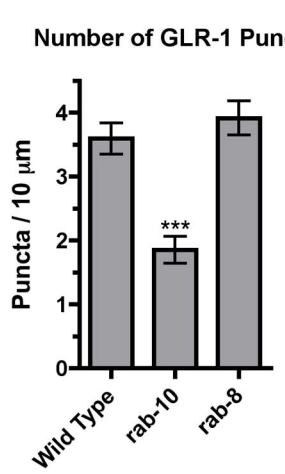
E
Number of GLR-1 Puncta
Puncta / 10 µm
***
Wild Type
rab-10
rab-8

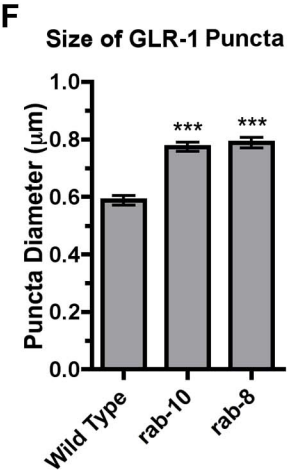
F
Size of GLR-1 Puncta
Puncta Diameter (µm)
***
***
Wild Type
rab-10
rab-8

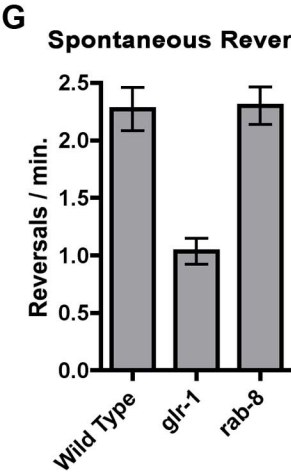
G
Spontaneous Reversals
Reversals / min.
Wild Type
glr-1
rab-8

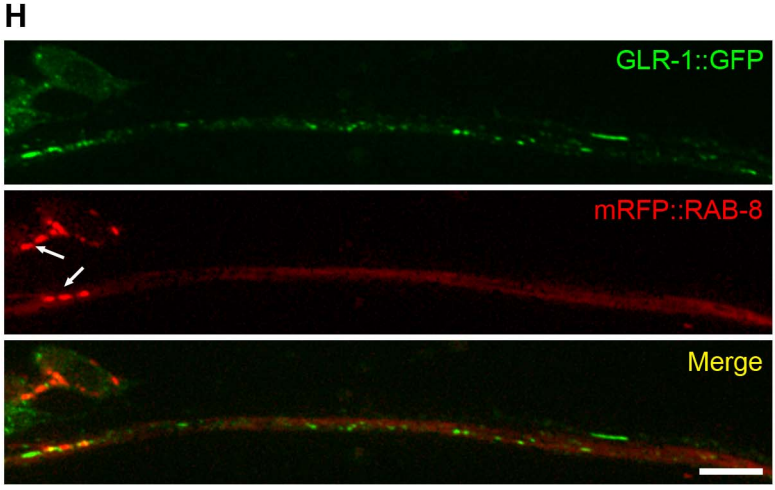
H
GLR-1::GFP
mRFP::RAB-8
Merge

WT

rab-10(q373)

rab-8 RNAi

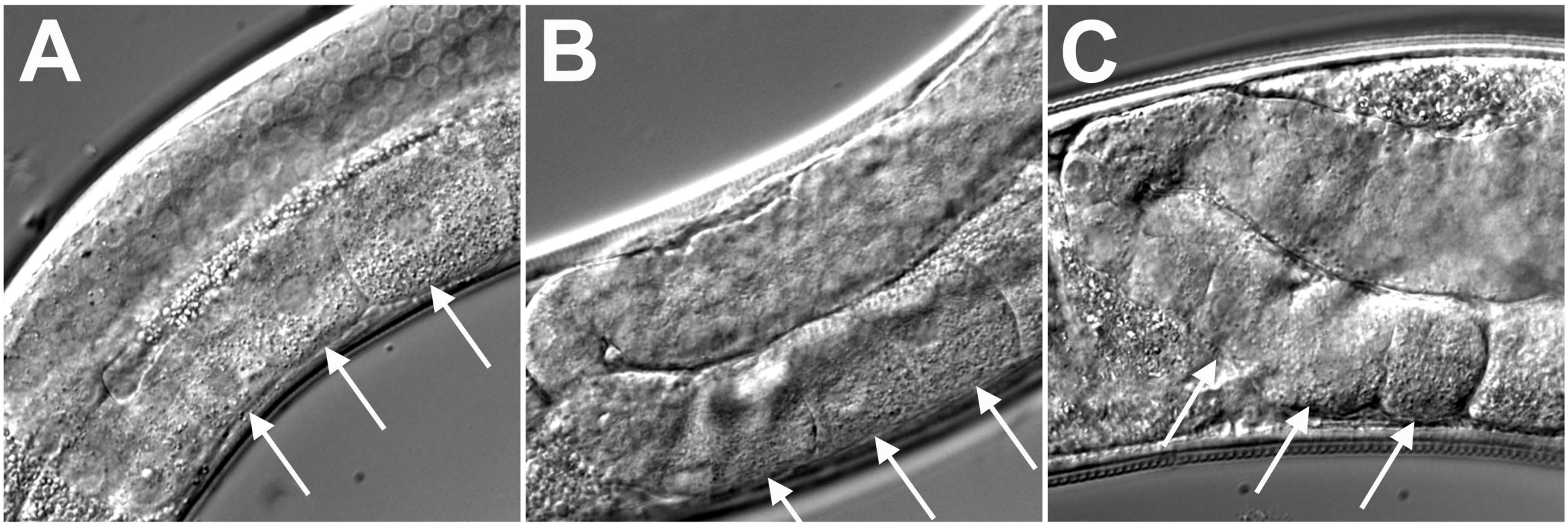

rab-10(q373);rab-8 RNAi

ehbp-1(tm2523)

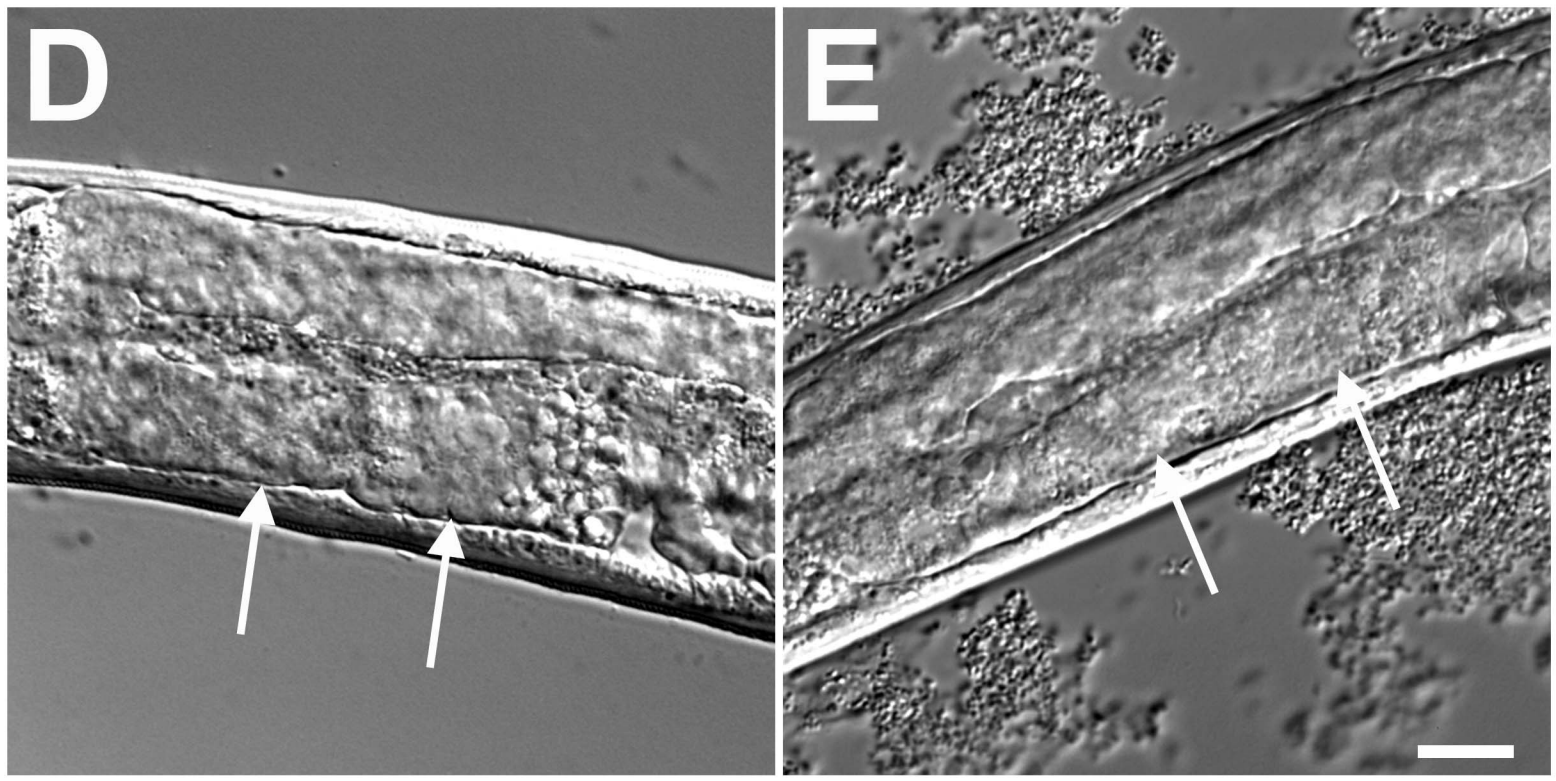

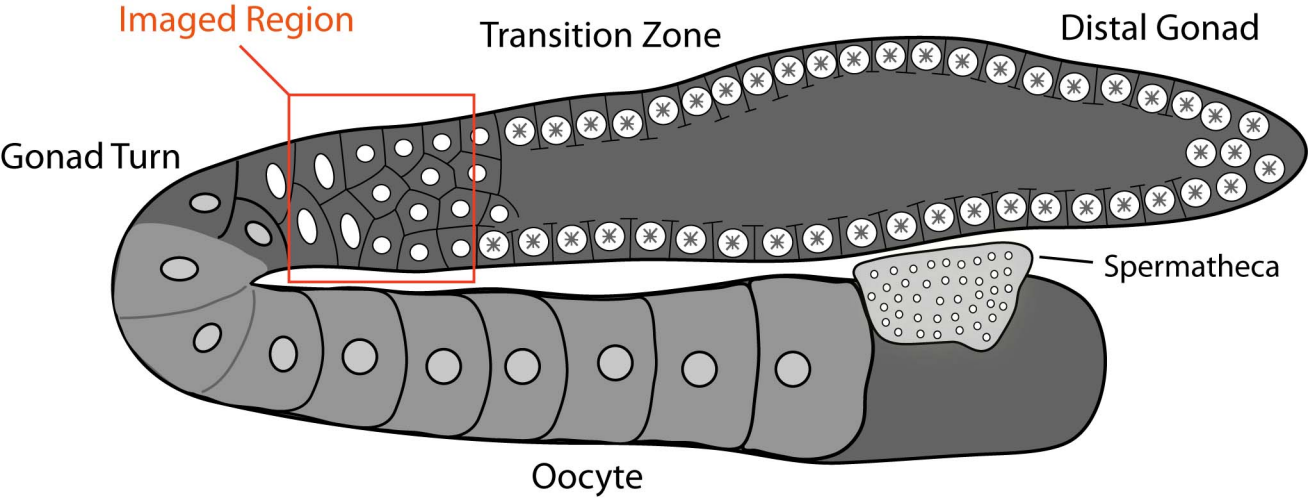
Imaged Region
Transition Zone
Distal Gonad
Gonad Turn
Spermatheca
Oocyte

Supplemental Table 1

Transgenic and Mutant Strains Used in This Study
*pwIs451[*p*ehbp-1::EHBP-1::GFP]*
*pwIs666[*p*vha6::EHBP-1::GFP]*
*pwIs846[*p*vha6::RFP::RAB-5]*
*pwIs414[*p*vha6::RFP::RAB-10](Chen et al., 2006)*
*pwIs500[*p*vha6:: RFP::RAB-8]*
*pwIs852[*p*vha6:: RFP::RME-1]*
*pwIs428[*p*vha6::RFP::RAB-11](Chen et al., 2006)*
*pwEx102[*p*vha6::MANS::RFP](Shi et al., 2007)*
*bIs1[*p*vit-2::GFP, rol-6(su1006)](Grant and Hirsh, 1999)*
*arIs37[*p*myo3::ssGFP, dpy-20(+)](Fares and Greenwald, 2001)*
*pwIs112[*p*vha6::hTAC::GFP](Chen et al., 2006)*
*pwIs90[*p*vha6::hTfR::GFP](Chen et al., 2006)*
*pwIs87[*p*vha6::GFP::RME-1](Chen et al., 2006)*
*pwIs72[*p*vha6::GFP::RAB-5](Chen et al., 2006)*
*pwIs206[*p*vha6::GFP::RAB-10](Chen et al., 2006)*
*pwIs69[*p*vha6::GFP::RAB-11](Chen et al., 2006)*
*pwIs68[*p*vha6::GFP::RAB-8*]
*pwIs883[*p*vha6::EHBP-1::mCherry]*
*pwIs888[*p*vha6::EHBP-1(1-711)::mCherry]*
*nuIs25[*p*glr-1::GLR-1::GFP*](Glodowski *et al.*, 2007)
*odIs42[*p*glr-1::RFP::RAB-10*](Glodowski *et al.*, 2007)
*odEx [*p*glr-1::EHBP-1::GFP*]
*odIs1[*p*glr-1::SNB-1::GFP](Glodowski et al., 2007)*
*odEx[*p*glr-1::RFP::RAB-8]*
p*pie-1::mCherry::PH*$^{PLC1\delta1}$ *(Kachur et al., 2008)*
p*pie-1::SNB-1::GFP*
glr-1(ky176) (From C. elegans Gene Knockout Consortium)
rme-1(b1045)(Grant et al., 2001)
rab-10(q373)(Chen et al., 2006)
ehbp-1(tm2523) (kindly provided by Dr. Shohei Mitani, Japanese National Bioresource Project for the Experimental Animal "Nematode *C. elegans*"*)*

References

Chen, C.C., Schweinsberg, P.J., Vashist, S., Mareiniss, D.P., Lambie, E.J., and Grant, B.D. (2006). RAB-10 is required for endocytic recycling in the Caenorhabditis elegans intestine. Mol Biol Cell *17*, 1286-1297.

Fares, H., and Greenwald, I. (2001). Genetic analysis of endocytosis in Caenorhabditis elegans: coelomocyte uptake defective mutants. Genetics *159*, 133-145.

Glodowski, D.R., Chen, C.C., Schaefer, H., Grant, B.D., and Rongo, C. (2007). RAB-10 regulates glutamate receptor recycling in a cholesterol-dependent endocytosis pathway. Mol Biol Cell *18*, 4387-4396.

Grant, B., and Hirsh, D. (1999). Receptor-mediated endocytosis in the Caenorhabditis elegans oocyte. Mol Biol Cell *10*, 4311-4326.

Grant, B., Zhang, Y., Paupard, M.C., Lin, S.X., Hall, D.H., and Hirsh, D. (2001). Evidence that RME-1, a conserved C. elegans EH-domain protein, functions in endocytic recycling. Nat Cell Biol *3*, 573-579.

Kachur, T.M., Audhya, A., and Pilgrim, D.B. (2008). UNC-45 is required for NMY-2 contractile function in early embryonic polarity establishment and germline cellularization in C. elegans. Dev Biol *314*, 287-299.

Shi, A., Pant, S., Balklava, Z., Chen, C.C., Figueroa, V., and Grant, B.D. (2007). A novel requirement for C. elegans Alix/ALX-1 in RME-1-mediated membrane transport. Curr Biol *17*, 1913-1924.